# ARTICLE IN PRESS

Mechanical Systems and Signal Processing ■ (■■■) ■■■-■■■



Contents lists available at ScienceDirect

# Mechanical Systems and Signal Processing

journal homepage: www.elsevier.com/locate/jnlabr/ymssp



# Excitation design for damage detection using iterative adjoint-based optimization—Part 2: Experimental demonstration

M.T. Bement a,\*, T.R. Bewley b

#### ARTICLE INFO

Article history: Received 3 January 2008 Received in revised form 27 June 2008 Accepted 16 July 2008

Keywords: Adjoint Damage detection Structural health monitoring Optimization

#### ABSTRACT

The iterative, adjoint-based excitation optimization technique developed in Part 1 is evaluated on an experimental structure consisting of a non-linear cantilever beam. The developed technique is shown to be effective at producing excitations which significantly improve the detectability of damage relative to two different "naive" excitations (a random input and a chirp). The technique is also demonstrated to be effective across multiple damage levels. In addition, by formulating a second-order version of the adjoint problem, it is shown that the terms needed to solve the associated adjoint equation are readily available from many commercially available finite element packages, which further enhances the usability of the technique.

© 2008 Elsevier Ltd. All rights reserved.

#### 1. Introduction

In Part 1 [1] of this two-part paper, a technique was developed to optimize the excitation to a system for the purpose of making damage most visible. In this second part, the focus is on experimental validation of the developed technique on a structural system. In addition, a second-order version of the adjoint problem is formulated. Through this formulation, it is easily seen that the mass, damping, and tangent stiffness matrices are the only terms needed for the solution of the adjoint system. These matrices are calculated automatically by most commercial finite element codes, which enhances the usability of the developed technique.

One of the conjectures made in Part 1 was the robustness of the technique to modeling errors. The specific topic of robustness is not directly addressed in this paper. However, the experimental validation of the developed techniques is very important, because it lends support to this conjecture and demonstrates that the technique can be used in the real world, where modeling errors are inevitable.

The remainder of this paper describes the experimental setup, develops the appropriate adjoint problem for the excitation optimization, and presents the experimental results.

# 2. Experimental setup

The experimental setup consists of a non-linear cantilever beam, shown in Fig. 1. The beam, made from 6061 aluminum, is 381 mm long, 50.8 mm wide, and 2.29 mm thick. The nonlinearity is introduced through a set of neodymium magnets at the free end of the beam (region 1 in Fig. 1). A close up view of the magnets, with polarity annotations, is shown in Fig. 2.

0888-3270/\$ - see front matter @ 2008 Elsevier Ltd. All rights reserved. doi:10.1016/j.ymssp.2008.07.005

<sup>&</sup>lt;sup>a</sup> Los Alamos National Laboratory. USA

<sup>&</sup>lt;sup>b</sup> University of California at San Diego, USA

<sup>\*</sup> Corresponding author. Tel.: +1505 664 0098; fax: +1505 663 5225. E-mail address: bement@lanl.gov (M.T. Bement).

M.T. Bement, T.R. Bewley / Mechanical Systems and Signal Processing ■ (■■■) ■■■■■



Fig. 1. Experimental setup.

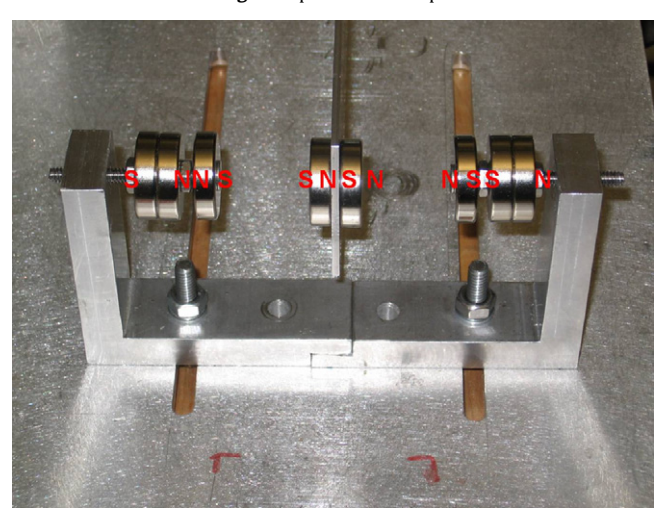


Fig. 2. Magnet configuration and orientation.

The magnets are arranged such as to create the effect of a stiffening spring between the free end of the beam and ground. As is discussed below, the magnets introduce a linear stiffness term in addition to non-linear terms. The purpose of the two magnets furthest from the beam and their associated orientation is to minimize this linear term. Damage is simulated by moving the magnets connected to ground further away from the beam. This has the effect of decreasing the stiffening effect. Excitation to the beam is provided by an electrodynamic shaker (region 2 in Fig. 1) located 130.5 mm from the clamped end. Beam deflection approximately half way in between the point of excitation and the free end of the beam is measured with a laser displacement sensor (region 3 in Fig. 1). The reason for choosing this location for measuring the displacement is due to the range and resolution of the laser displacement sensor. Thus, the goal of the excitation design is to provide an excitation that causes the undamaged and damaged measured displacements to be as different as possible.

# 3. Adjoint model development

The beam is modeled as an Euler-Bernoulli beam, and is governed by the familiar equation

$$\begin{split} \frac{d^2}{dx^2} \left( EI \frac{\partial^2 u}{\partial x^2} \right) + \rho A \frac{\partial^2 u}{\partial t^2} &= 0 \\ u(0,t) &= \frac{\partial u}{\partial x}(0,t) = 0 \\ \frac{d}{dx} \left( EI \frac{d^2 u}{dx^2} \right) \bigg|_{x=x_s} &= f(t) \\ \frac{d}{dx} \left( EI \frac{d^2 u}{dx^2} \right) \bigg|_{x=t_s} &= k_{nl_1} u(L,t) + k_{nl_3} u(L,t)^3 + k_{nl_5} u(L,t)^5 \end{split}$$

M.T. Bement, T.R. Bewley / Mechanical Systems and Signal Processing ■ (■■■) ■■■■■■

where u is the defection of the beam, E is the elastic modulus, I is the area moment of inertia,  $\rho$  is the density per unit length, A is the cross sectional area, E is the length of the beam, E is the force supplied by the shaker, and E is the location of the shaker. The boundary condition at the free end due to the magnets can be easily derived. The force between two parallel magnets decreases with one over distance to the fourth power. Because there are magnets on both sides of the beams, the force seen at the free end of the beam due to the magnets may be modeled as

$$f(u(L)) = \operatorname{sgn}(u(L) - d) \frac{k_{\text{mag}}}{(u(L) - d)^4} + \operatorname{sgn}(u(L) + d) \frac{k_{\text{mag}}}{(u(L) + d)^4}$$
(1)

where  $k_{\rm mag}$  is a coefficient related to the strength of the magnets and d is distance between the magnets on the beam and the ones attached to ground. Force/displacement data were collected for the undamaged configuration ( $d=0.035\,{\rm m}$ ). From these data, it was determined that  $k_{\rm mag}=2.7e-6\,{\rm N}\,{\rm m}^4$ . Furthermore, for reasons relating to the solution of the equations, this model was approximated with a fifth-order polynomial. Because of the symmetric nature of the force/displacement function, the constant, second, and fourth-order coefficients in this polynomial fit are zero and  $k_{nl_1}$ ,  $k_{nl_3}$ , and  $k_{nl_5}$  are the first, third, and fifth-order coefficients, respectively. Note that despite the non-linear nature of the magnets, they do introduce a linear stiffness component. Fig. 3 shows the experimental data, the fit from the model, and the polynomial fit.

The magnets attached to the free end of the beam have a mass of  $43.6 \, \text{g}$ , and it is assumed that the shaker introduces an additional mass, stiffness and damping at its point of application. The mass is taken to be  $50 \, \text{g}$ , the stiffness is taken to be  $18 \, \text{kN/m}$ , and the damping is taken to be  $70 \, \text{N/m/s}$ . This equation is solved using a standard finite element method (cubic Hermite shape functions) with 20 elements (see, for example [2]). This results in a set of ODEs of the form

$$M\ddot{U} + C\dot{U} + K(u)U = Bf(t) \tag{2}$$

where  $U = [u^T (du/dx)^T]^T$ . Because it will be used below, we also note that the tangent linear equation can be easily verified to be given by

$$M\ddot{U}' + C\dot{U}' + K(t)U' = Bf'(t) \tag{3}$$

Because the stable time step necessary for integration of this set of equations using the fourth-order Runge–Kutta method is very small (less than a microsecond), Eq. (2) is integrated in time using the Newmark method with constant average acceleration

$$\begin{split} &U_{k+1} = U_k + \Delta \dot{U}_k + 0.5 (\Delta t)^2 \ddot{U}_{k+0.5} \\ &\dot{U}_{k+1} = \dot{U}_k + \Delta t \ddot{U}_{k+0.5} \\ &\ddot{U}_{k+0.5} = 0.5 \ddot{U}_k + 0.5 \ddot{U}_{k+1} \end{split}$$

With this integration scheme, much larger time steps are possible (1 ms was chosen). Let the output y = GU be the deflection at the location of the laser displacement sensor (approximately 247 mm from the clamped end). Following the procedure developed in Part 1, the cost function that we seek to maximize is

$$J = \frac{1}{2} \int_0^T (y_u - y_d)^T (y_u - y_d) dt = \frac{1}{2} \int_0^T (\overline{GU})^T \overline{GU} dt = \frac{1}{2} \int_0^T \overline{U}^T \overline{QU} dt$$
 (4)

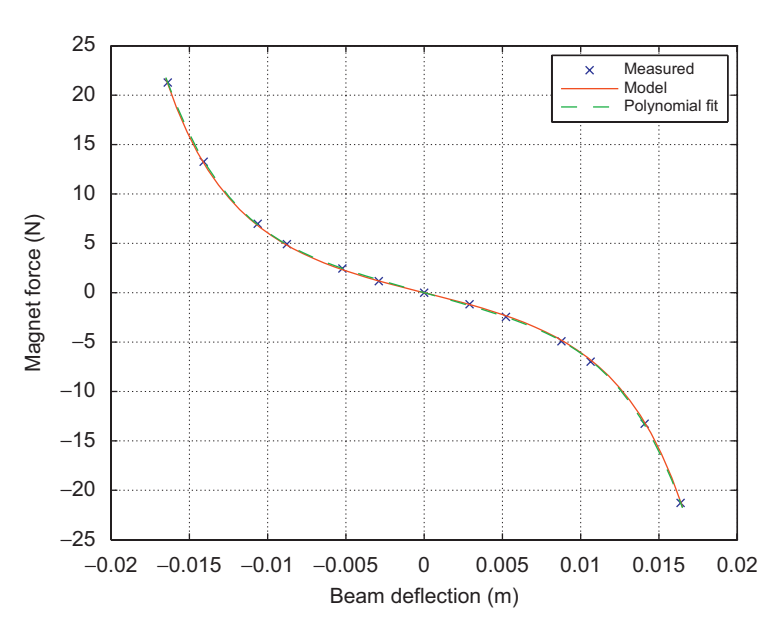


Fig. 3. Magnet force/displacement data for undamaged configuration.

4

where  $y_u$  represents the output for the undamaged condition,  $V_d$  represents the output for the damaged condition,  $\overline{U} = [U_u^T \ U_d^T]^T$ ,  $\overline{G} = [G \ -G]$ , and  $\overline{Q} = \overline{G}^T \overline{G}$ . Following the technique developed in Part 1, which is not repeated here, it is seen that the second-order version of the adjoint equation is given by

$$\overline{M}^T \ddot{R} - \overline{C}^T \dot{R} + \overline{K}^T R = \overline{OU}$$

$$R(T) = 0$$

where

$$\overline{M} = \begin{bmatrix} M & 0 \\ 0 & M \end{bmatrix}, \quad \overline{C} = \begin{bmatrix} C & 0 \\ 0 & C \end{bmatrix}, \quad \overline{K} = \begin{bmatrix} K_u(t) & 0 \\ 0 & K_d(t) \end{bmatrix}$$

and  $K_u(t)$  and  $K_d(t)$  are the time varying stiffness matrices obtained from the tangent linear equations for the undamaged and damaged systems, respectively. It is worth noting that the adjoint equation only requires the mass, damping and tangent stiffness matrices, all of which are available in any number of commercial finite element codes. Thus, a commercial finite element code such as Abaqus could be used, without the need for any special, adjoint version of the code. This represents a significant usability advantage. The gradient of the cost function with respect to the excitation f(t) then follows from Part 1 and is given by

$$\frac{DJ}{Df} = R^T \overline{B}$$

where  $\overline{B} = [B^T \ B^T]^T$ . The updated excitation is then given by

$$f(t)_{n+1} = f(t)_n + \alpha \frac{DJ}{Df}$$

where  $\alpha$  is determined via a line search. This updated f(t) is then normalized to the maximum excitation amplitude, as appropriate. For this example, the excitation supplied to the shaker was limited to 10 V.

### 4. Results

Two different damage scenarios were considered. The first, referred to as damage scenario 1, corresponds to moving the magnets attached to ground away from the beam by 3.1 mm. For the second scenario, referred to as damage scenario 2, the first damaged state becomes the new "undamaged" system, and damage corresponds to moving the magnets attached to ground an additional 1.4 mm away from the beam. Using Eq. (1), we can predict the magnet force (and associated polynomial fit coefficients) for these damage scenarios by altering d (by 38.3 mm for the first scenario and 39.7 mm for the second scenario). A plot of the resulting magnet force/displacement curves is shown in Fig. 4.

Following the same procedure as in Part 1, we select a random input with frequency content up to 30 Hz as the initial excitation. The duration of the excitation, *T*, was chosen to be 2 s, and the sampling frequency used was 1000 Hz. Because

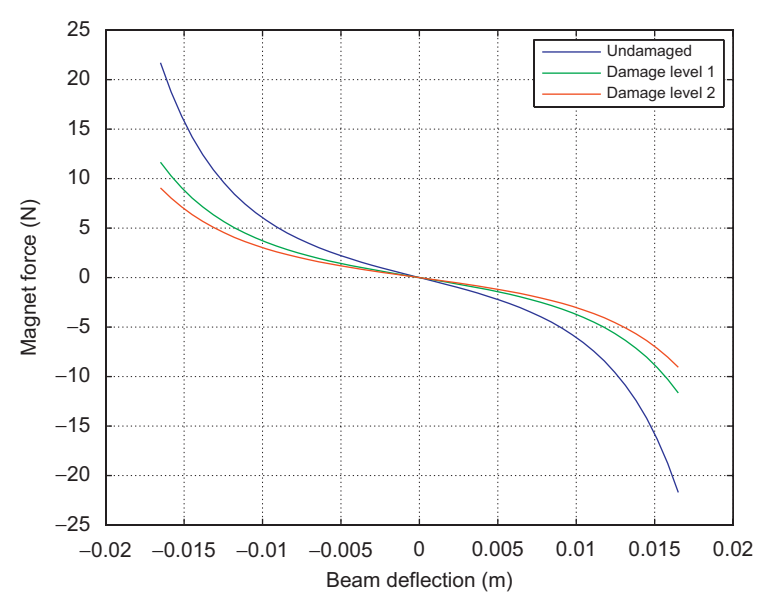


Fig. 4. Magnet force/displacement data.

the bandwidth of the electrodynamic shaker is approximately 5000 Hz, no actuator dynamics needed to be incorporated into the damaged and undamaged models. A plot of this initial excitation is shown in Fig. 5.

The predicted cost function (4) was evaluated for both damage scenarios using this initial excitation, and the procedure outlined above and in Part 1 was followed to optimize the excitation for each damage scenario. The initial and optimized signals (which were limited to 10 V) were then supplied to the shaker, and the response recorded. From this recorded response, actual values of the cost function may be calculated to determine if indeed the optimized excitation gave a larger value of the cost function than the initial excitation.

For the first damage scenario, the predicted cost function value for the initial random excitation signal is 1.2e - 7. The optimized excitation for this scenario is shown in Fig. 6 and will be referred to as E1. The predicted cost function value for the E1 excitation is F1.1e - 6 (approximately a F1.1e - 6) increase as compared to the random excitation).

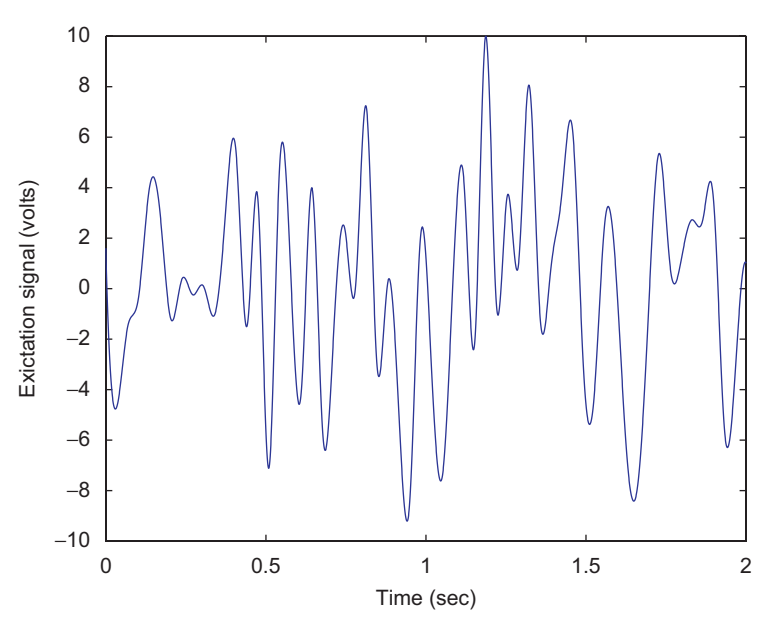


Fig. 5. Initial random excitation.

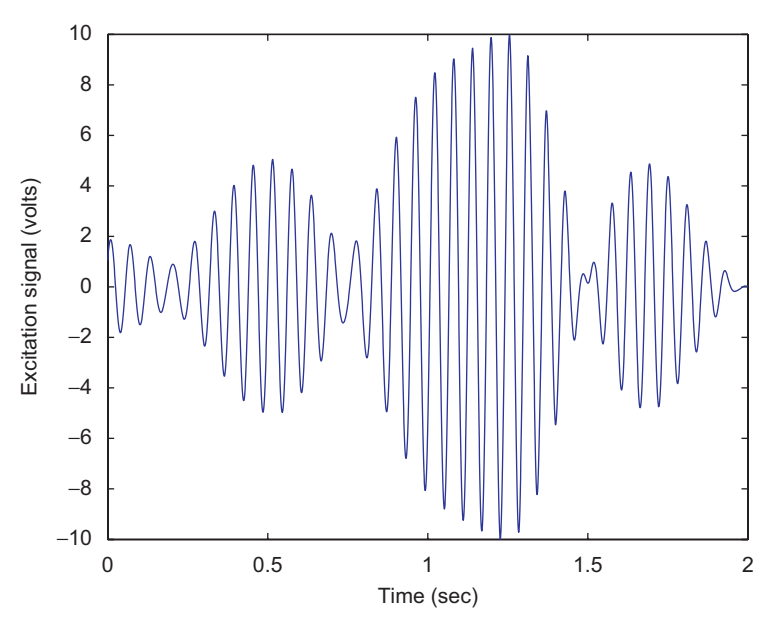


Fig. 6. Damage scenario 1 optimized excitation.

The actual cost function value for the random excitation is 1.1e-7, and the actual cost function value for the E1 excitation is 7.1e-6 (approximately a  $62 \times$  increase as compared to the random excitation). Fig. 7 shows  $y_u - y_d$  for the chirp and E1 excitations, and the increased difference due to the E1 excitation is clearly visible.

For the second damage scenario (which is essentially designing an excitation to tell the difference between damage level 1 and damage level 2), the predicted cost function value for the random excitation is 1.3e-7, and the predicted cost function value for the optimized excitation is 7.5e-6 (approximately a factor of  $58 \times$  improvement as compared to the random excitation). The optimized excitation for this damage scenario is shown in Fig. 8 and will be referred to as E2.

The actual cost function value for the random excitation is 6.7e-8, and the actual cost function value for the E2 excitation is 2.0e-6 (approximately a  $30\times$  increase as compared to the random excitation). Fig. 9 shows  $y_u-y_d$  for the chirp and E2 excitations.

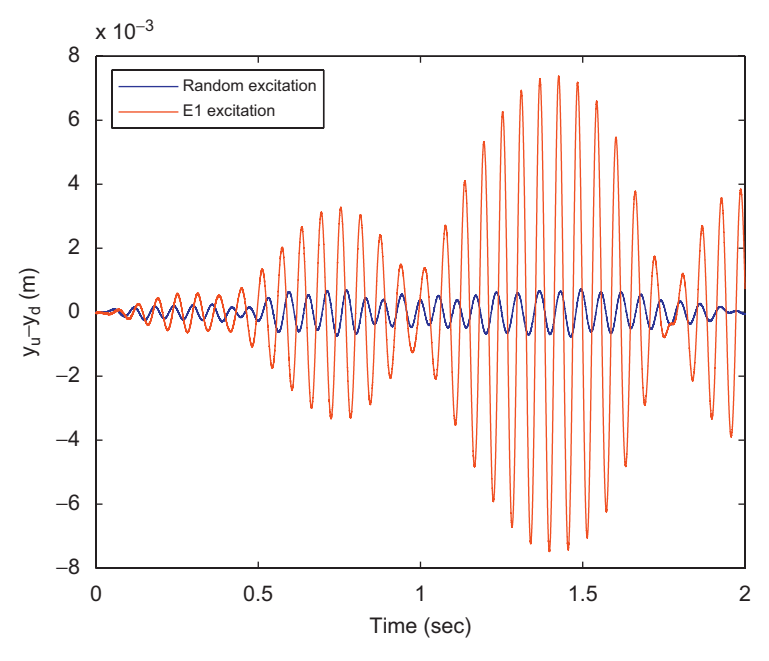


Fig. 7. Damage scenario 1 response to random and optimized excitation E1.

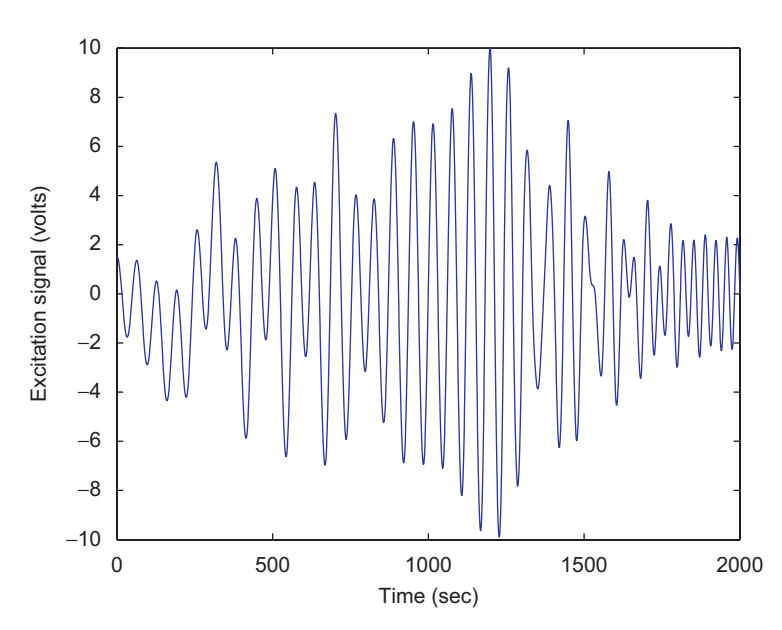


Fig. 8. Damage scenario 2 optimized excitation.

M.T. Bement, T.R. Bewley / Mechanical Systems and Signal Processing ■ (■■■) ■■■■■■

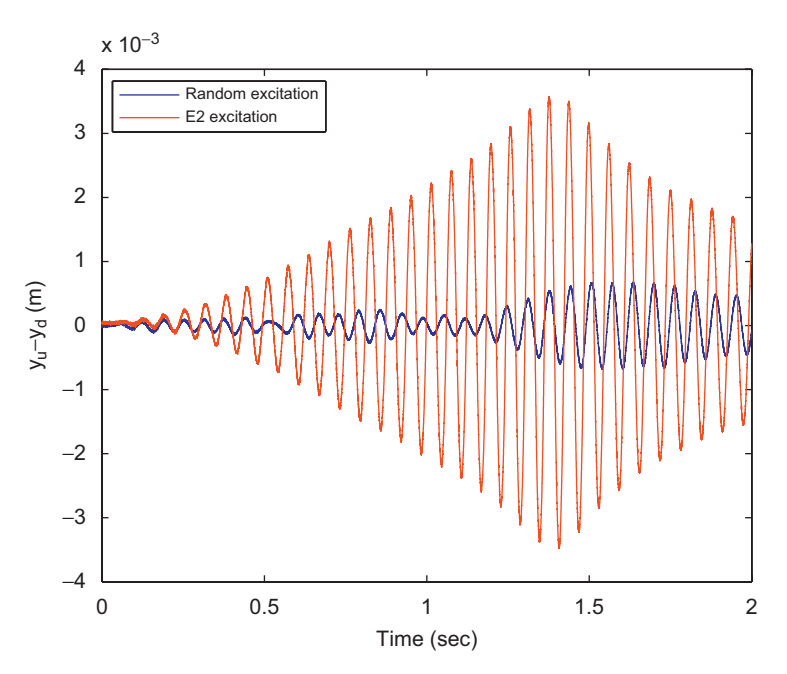


Fig. 9. Damage scenario 2 response to random and optimized excitation E2.

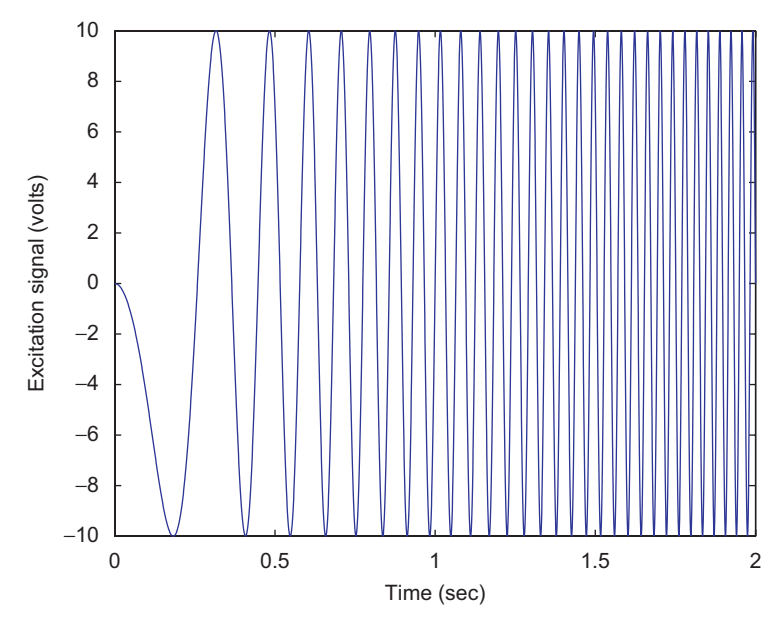


Fig. 10. Initial chirp excitation.

In the Example in Part 1, it was seen that a random input was not as good of an input as a sinusoid. For the sake of completeness, and to demonstrate that the developed technique does not just improve on very poor initial excitations, it is desirable to compare the optimized excitations to a sinusoidal excitation. However, because the magnets introduce a linear stiffness component at the free end of the beam (in addition to the non-linear components), it is not as straightforward as that in the Example in Part 1 to select a meaningful single frequency sinusoid to use as the initial excitation. As a compromise, a chirp signal from 0 to 30 Hz was selected as an alternate initial excitation. This initial excitation is shown in Fig. 10.

The predicted and observed values for the cost function for the chirp signal, and the optimized signals for both damage levels are summarized in Table 1. Plots of  $y_u - y_d$  for these excitations are shown in Figs. 11 and 12. Clearly, the optimized excitations are still an improvement, even compared to the chirp excitation. Finally, for the sake of completeness, the

**Table 1**Results with chirp excitation

	Predicted J (chirp)	Actual J (chirp)	Predicted <i>J</i> ( <i>E</i> )	Actual $J(E)$
Damage scenario 1	2.6e – 6	3.0e - 6	7.1e – 6	7.1e – 6
Damage scenario 2	1.3e – 6	0.8e - 6	7.5e – 6	2.0e – 6

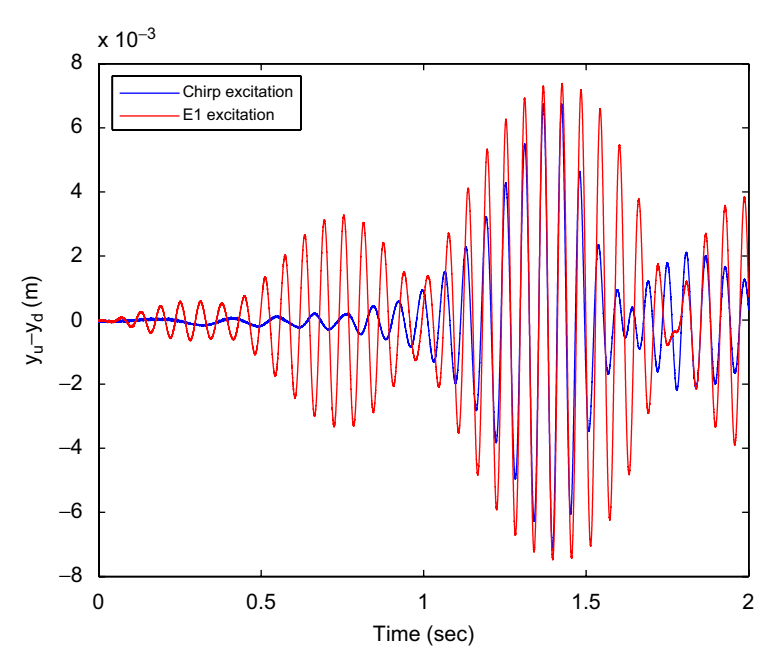


**Fig. 11.** Damage scenario 1 response to chirp and optimized excitation *E*1.

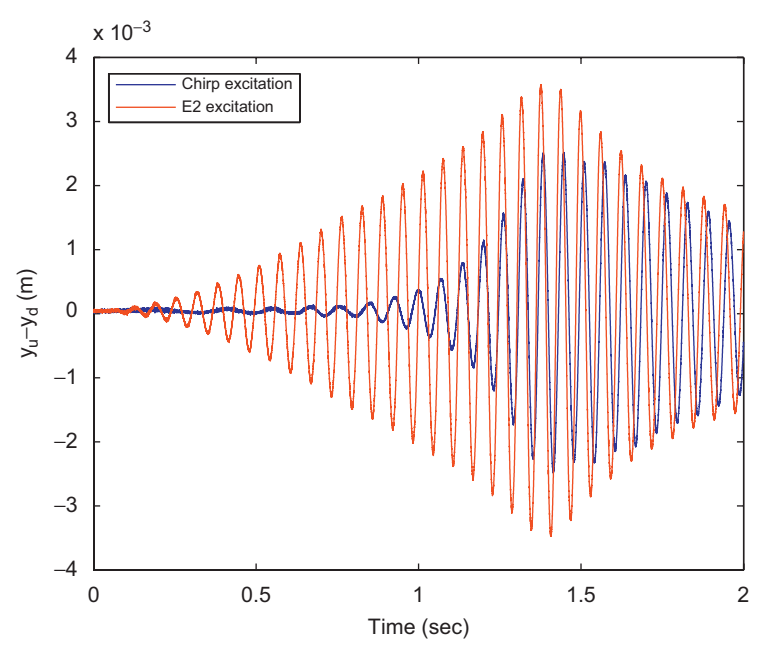


Fig. 12. Damage scenario 2 response to chirp and optimized excitation E2.

M.T. Bement, T.R. Bewley / Mechanical Systems and Signal Processing ■ (■■■) ■■■■■■

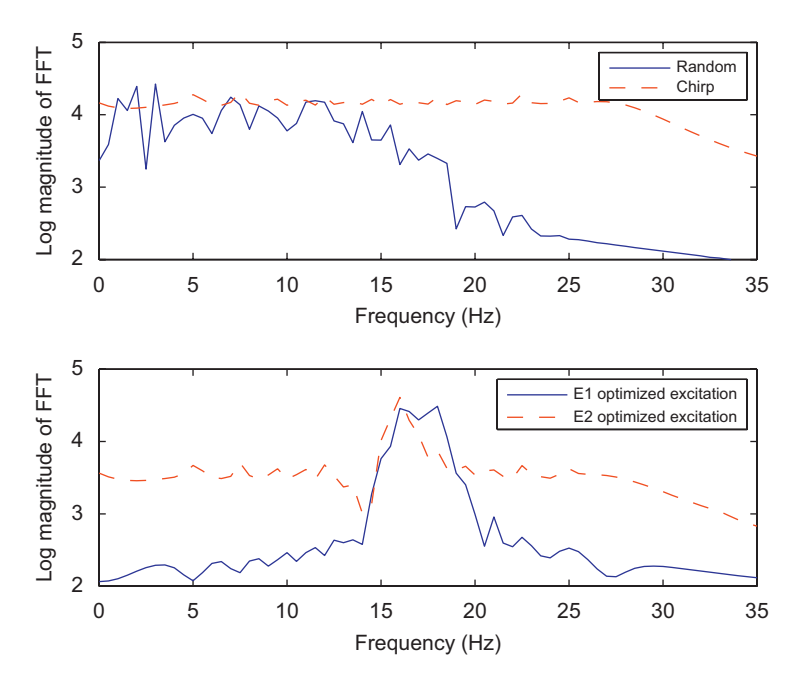


Fig. 13. Log magnitudes of excitations in frequency domain.

log-magnitude in the frequency domain of all excitations is shown in Fig. 13. This figure is given purely for comparison purposes, as it is emphasized that the developed excitation optimization technique is a time domain technique and makes no statements about the frequency characteristics of the optimized signal.

# 5. Discussion and recommendations for future research

There are several aspects of the results worthy of discussion. First, the developed technique was shown to produce excitations which improve the detectability of damage relative to two different "naive" excitations (a random input and a chirp). In addition, the technique was shown to be effective across multiple damage levels. While not surprising, it is interesting to note that the excitation produced for damage scenario 2 was not the same as the excitation produced for damage scenario 1. Indeed, even to the eye, the excitations look significantly different. This implies that the excitation that is useful for identifying one type of damage need not be the same as the excitation useful for identifying a different or subsequent type of damage. This is actually quite a useful effect as it may be possible to design an excitation which is sensitive to one type of change (e.g., damage), but is not sensitive to other types of change (e.g., temperature change). Because the so-called "data normalization" is a significant challenge in structural health monitoring, this "selective" excitation design represents an interesting area for future research.

It is also interesting to note that while the designed excitations undeniably improve the detectability of the damage relative to the naive excitations, the prediction of this improvement in damage scenario 1 was more accurate than the prediction of this improvement in damage scenario 2. There may be several reasons for the discrepancy. One possible reason may be incorrect modeling of the magnets for the second damage scenario. Recall that the terms in Eq. (1) were fit using force/displacement data obtained in the undamaged condition. The damaged conditions were then estimated by increasing d in Eq. (1). However, as d increases, the magnets on the beam and the magnets attached to ground become less parallel when they come into close proximity, due to the slope at the free end of the beam. Because Eq. (1) is only valid for parallel magnets, the model for the magnetic force may start to lose accuracy at higher damage levels. If the model for damage is incorrect, it should come as no surprise if the predicted and actual values for the increase in the cost function for the designed excitation are somewhat different.

Regardless of whether the damage model is correct, there are certainly other modeling errors. For example, other than attempting to capture effective mass, damping, and stiffness terms for the shaker, no other shaker or amplifier dynamics were modeled. In Part 1, a conjecture was made that the developed technique should be somewhat insensitive to non-damage related modeling errors. The fact that the prediction for the increases in the cost function for damage scenario 1 was quite accurate supports this conjecture. To understand another potential reason for the discrepancy in the magnitude of the predicted effect for damage scenario 2, recall that as noted above, the excitation for damage scenario 1 and the excitation for damage scenario 2 appears to be significantly different. Thus, it may be possible that some excitations are

# ARTICLE IN PRESS

M.T. Bement, T.R. Bewley / Mechanical Systems and Signal Processing ■ (■■■) ■■■■■■

more robust to non-damage related modeling errors than other excitations. A formal investigation into designing "robust" excitation represents another area for future research.

## 6. Conclusions

The iterative, adjoint-based excitation optimization technique developed in Part 1 was evaluated on an experimental structure consisting of a non-linear cantilever beam. The developed technique was shown to be effective at producing excitations which significantly improve the detectability of damage relative to two different "naive" excitations (a random input and a chirp). The technique was also shown to be effective across multiple damage levels. In addition, by formulating a second-order version of the adjoint problem, it was shown that the terms needed to solve the associated adjoint equation are readily available from many commercially available finite element packages, which further enhances the usability of the technique. Finally, avenues for future research including "selective" excitation design and "robust" excitation design were proposed.

# References

[1] M.T. Bement, T.R. Bewley, Excitation design for damage detection using iterative adjoint-based optimization—part 1: Method development, Mechanical Systems and Signal Processing, 2008, in press. doi:10.1016/j.ymssp.2008.07.006.

[2] J.N. Reddy, An Introduction to the Finite Element Method, second ed., McGraw-Hill, New York, 1993.

10